



Published in final edited form as:

Nature. 2011 January 20; 469(7330): 415–418. doi:10.1038/nature09637.

## Paneth cells constitute the niche for Lgr5 stem cells in intestinal crypts

Toshiro Sato, Johan H. van Es, Hugo J. Snippert, Daniel E. Stange, Robert G. Vries, Maaike van den Born, Nick Barker, Noah F. Shroyer<sup>1</sup>, Marc van de Wetering, and Hans Clevers

Hubrecht Institute, Uppsalalaan 8, 3584CT Utrecht, the Netherlands <sup>1</sup>Cincinnati Children's Hosp, Div Gastroenterology, Med Ctr, MLC 2010,3333 Burnet Ave, Cincinnati, OH 45229 USA

### Abstract

Homeostasis of self-renewing small intestinal crypts results from neutral competition between Lgr5 stem cells, small cycling cells located at crypt bottoms<sup>1,2</sup>. Lgr5 stem cells are interspersed between terminally differentiated Paneth cells, that are known to produce bactericidal products such as lysozyme and cryptidins/defensins<sup>3</sup>. Single Lgr5-expressing stem cells can be cultured to form long-lived, self-organizing crypt-villus organoids in the absence of non-epithelial niche cells<sup>4</sup>. Here, we note a close physical association of Lgr5 stem cells with Paneth cells *in vivo* and *in vitro*. CD24<sup>+</sup> Paneth cells express EGF, TGF $\alpha$ , Wnt3 and the Notch-ligand Dll4, all essential signals for stem cell maintenance in culture. Co-culturing of sorted stem cells with Paneth cells dramatically improves organoid formation. This Paneth cell requirement can be substituted by a pulse of exogenous Wnt. Genetic removal of Paneth cells *in vivo* results in the concomitant loss of Lgr5 stem cells. In colon crypts, CD24<sup>+</sup> cells residing between Lgr5 stem cells may represent the Paneth cell equivalents. We conclude that Lgr5 stem cells compete for essential niche signals provided by a specialized daughter cell, the Paneth cell.

In a Matrigel-based culture system containing EGF, the Wnt agonist Rspodin1 and the BMP inhibitor Noggin<sup>4</sup>, single Lgr5 stem cells autonomously grow into crypt-like structures with *de novo* generated stem cells and Paneth cells at their bottom. The remainder of these crypts consists of transit-amplifying cells, which feed into villus-like luminal domains containing post-mitotic enterocytes and goblet cells. Thus, a single Lgr5 intestinal stem cell can generate a continuously expanding, self-organizing organoids reminiscent of normal gut in the absence of a subepithelial cellular niche. Confocal cross-sectioning of crypt bottoms of *Lgr5-EGFP-ires-CreERT2* mice revealed an almost geometrical distribution of Paneth cells and Lgr5 stem cells, that maximized heterotypic contact area (Paneth-stem cell) and minimized homotypic contact area (Fig 1a-c). The same intimate contact was observed in the organoid cultures at crypt bottoms (Fig 1d and Suppl Movie 1).

The hypothesis that Paneth cells supply essential niche signals was rejected previously<sup>5</sup>. To retest this, stem cells sorted from *Lgr5-EGFP-ires-CreERT2* mice based on GFP expression<sup>6</sup>, were recombined with wild type Paneth cells sorted for CD24 expression (Fig 2a/c). Of note, CD24-expressing cells reside between Lgr5 stem cells in colon crypts (Fig 2b), suggesting that these are related to Paneth cells. Indeed, a secretory cell type –distinct from goblet cells–resides at colon crypt bottoms<sup>7</sup>. Stem cells and/or Paneth cells were seeded in round-bottom plates in 10% Matrigel. Reassociated Lgr5 stem cells typically formed

### Declaration of competing financial interests

H.C. is an inventor on several patents involving the culture system in this paper, as is T.S.

short-lived, cystic clusters (Fig 2d). Reassociated Paneth cells tended to form larger aggregates (Fig 2e), which disintegrated after 5 days. In three independent experiments, long-lived GFP organoids were formed in only  $6.7 \pm 3.3\%$  of 10 wells per experiment containing 500 Lgr5 stem cells each, and in 0% of 10 wells per experiment containing 500 Paneth cells each (we occasionally observed GFP-negative organoids originating from contaminating wild type Paneth cells). When 500 stem cells and 500 Paneth cells were combined, GFP<sup>+</sup> organoids formed in  $76.7 \pm 8.8\%$  of 10 wells per experiment (Fig 2f/g). The dynamic reassociation process was illustrated using Lgr5<sup>+</sup> cells sorted from a clonal RFP<sup>+</sup> organoid culture and Paneth cells from a clonal YFP<sup>+</sup> organoid culture. As shown in a movie (Fig 2h and Suppl Movie 2), multiple cell clusters formed initially. The organoids fused to form one or two large organoids per well (Suppl Movie 2). Thus, Lgr5 stem cells and Paneth cells appeared to require physical contact. Indeed, Lgr5 stem cells are critically dependent on Notch signals<sup>8-10</sup>, which depend on direct cell-cell contact.

We then performed comparative gene expression profiling on stem and Paneth cells. The heat map in Fig 3a confirmed the segregation of Paneth cells markers (lysozyme, DefensinA1<sup>3</sup>) and stem cell markers (Lgr5, Olfm4, Tnfrsf19, CDCA7<sup>11</sup>). Amongst the genes most highly enriched in Paneth cells, we noted Wnt3 and Wnt11, EGF and TGF $\alpha$ , and the Notch ligand, Dll4 (Fig 3a). Wnt3 expression<sup>12</sup> and EGF expression<sup>13</sup> had been noted previously. Thus, Paneth cells provided essential signals for stem cell support: EGF, Wnt3 and Notch. High level expression of *Wnt3* was confirmed by *in situ* hybridization (Fig 3b).

Rspondin1 potentially amplifies Wnt responses, yet is inactive on its own<sup>14</sup>. When organoids were grown from crypts derived from the Axin2-LacZ mice<sup>15</sup>, Wnt responses as assayed by lacZ expression were restricted to the crypt base, despite the ubiquitous presence of Rspondin1 (Fig 3c/e, Suppl Fig 1). When exogenous Wnt3A was added, the organoids diffusely expressed the blue Wnt reporter (Fig 4g). The global response to Wnt caused the typical crypt-villus architecture to change into rounded cysts devoid of differentiated cell types (Fig 3e, g). Indeed, Wnt signaling instructs intestinal cells to adopt a proliferative progenitor phenotype<sup>16</sup>. The same rounded cysts were routinely observed upon culturing Apc deficient cells from *APC<sup>min</sup>* adenomas<sup>17</sup> (Fig 3d). When the small molecule Wnt secretion inhibitor (Porcupine inhibitor) IWP1<sup>18</sup> was added, the Axin2-LacZ signal in wt organoids was entirely lost and proliferation halted (Compare Fig 3e and f; a dose-response curve given in Suppl Fig 2). This inhibition could be overcome by exogenous Wnt3A (Fig 3g/h; Suppl Fig 2), confirming the specificity of the Wnt secretion inhibitor. We concluded that exogenous Rspondin1 acts by amplifying the local response to short-range Wnt produced by Paneth cells. Thus, only the direct neighbors of Paneth cells, the Lgr5 stem cells, receive strong Wnt signals, which can be further increased by Rspondin1. Moreover, these observations implied that the asymmetry of crypt-villus organoids was established by the localized presence of Wnt-producing Paneth cells. We recently observed that stem cell-Paneth cell doublets display a strongly increased plating efficiency compared to single stem cells<sup>2</sup>. This Paneth cell-dependence of single stem cells, illustrated in suppl Fig3, could be overcome by addition of Wnt-3A at 100 ng/ml for the first three days of culture (Fig 3i).

To investigate in *in vivo* models whether Paneth cells provide essential support to Lgr5 stem cells, we utilized three previously described genetic mouse models for Paneth cell loss: mutation of *Gfi1*<sup>19</sup>, transgenic expression of Diphtheria Toxin A under the Paneth cell-specific Cryptdin2 promoter (*CR2-tox176*) and conditional deletion of *Sox9*<sup>20,21</sup>. When we re-visited crypts of *Gfi1*<sup>-/-</sup> adult mice, described to lack Paneth cells<sup>19</sup>, Paneth cell numbers were reduced but not absent, as also seen recently<sup>22</sup>. Lysozyme staining revealed that the majority of crypts harbored at least one Paneth cell (Fig 4a-b; Suppl Fig 4; Sequential section analysis revealed that >90% of crypts possess more than one Paneth cells (not shown)). Stem cells were coincidentally decreased in number (Fig 4d-e) and colocalized with

remaining Paneth cells as visualized by double staining for *Olfm4* and Lysozyme (Fig 4g-h). Similarly, in the *CR2-tox176* mice, we noted that Paneth cells were reduced but present (Fig 4c; Suppl Fig 4) in agreement with the reported 82% decrease in Paneth cell numbers<sup>5</sup>. Numbers of stem cells were again decreased, coincident with Paneth cells (Fig4c, f, i-k).

We conditionally deleted the *Sox9* gene in 6-week old mice, homozygous for a *Sox9<sup>fllox</sup>* allele and heterozygous for the *Ah-Cre* allele<sup>23</sup>. Paneth cells are estimated to have a life-time of 8 weeks<sup>24</sup>. The *Sox9* gene was efficiently deleted in all crypt cells with the exception of pre-existing Paneth cells, where the *Ah-Cre* transgene is not activated<sup>23</sup>. Although *Sox9* is expressed in *Lgr5* stem cells<sup>11</sup>, we observed no stem cell phenotype at early time points post-deletion (Suppl Fig 5a/b). From 4 weeks onwards, Paneth cell numbers visibly decreased. Loss was virtually complete after 7-8 weeks (Fig 4s), after which a regenerative response occurred. We occasionally noted *Sox9*<sup>-/-</sup> crypts with a single remaining *Sox9*-positive Paneth cell (Suppl Fig 5c; red arrows). Stem cells disappeared coincident with Paneth cells, and remaining stem cells crowded around remaining Paneth cells (Suppl Fig 5d). Suppl. Fig 6 depicts a field of escaper wt crypts adjacent to a field of *Sox9*-negative crypts. The escaping wt crypts containing abundant Paneth cells rapidly replaced the mutant crypts by crypt fission (Suppl Fig 6). By day 67, all crypt basal cells were *Sox9*<sup>+</sup> again (Fig 4n) and contained normal numbers of Paneth cells (Fig 4t) and stem cells (Fig 4q). From this, we concluded that Paneth cells are essential for maintenance of crypts and stem cells.

Stem cell niches are typically portrayed as pre-existing sites, to which stem cells migrate<sup>25</sup>. Here we show that intestinal stem cells receive niche support from their own specialized progeny. This is not without precedent, as the somatic stem cells of the fly testis give rise to differentiated cells that in turn build the testis niche<sup>26</sup>. Thus, Paneth cells serve as multifunctional guardians of stem cells, both by secreting bactericidal products and by providing essential niche signals. *Lgr5* stem cells divide symmetrically and their numbers are restricted by neutral competition at the stem cell population level<sup>2</sup>. We now propose that the *Lgr5* stem cells compete for available Paneth cell surface. Paneth cell numbers must therefore be tightly regulated, which is indeed the case. Paneth cells are born directly above the crypt base, the latter originally termed the “stem cell zone”<sup>27,28</sup>. It will be of interest to understand what determines Paneth cell numbers and their slow turnover rate.

## Methods (On line version)

### Reagents

Murine recombinant EGF and Noggin (Peprotech). Murine recombinant Wnt-3a (Millipore). Human recombinant R-spondin 1 provided by Arie Abo<sup>29</sup>. Y-27632 (Sigma). IWP1 provided by Lawrence Lum<sup>18</sup>.

### Mice

*Lgr5-EGFP-Ires-CreERT2* mice<sup>1</sup>, *APC<sup>min17</sup>*, *Axin2-lacZ* mice<sup>15</sup>, *Gfi1*<sup>-/-19</sup>, *CR2-tox176*, *Sox9<sup>fl/fl20</sup>* and R26R-confetti<sup>2</sup> mice were described earlier. The transgenic *Ah-Cre* line<sup>23</sup> was crossed with *Sox9<sup>fl/fl</sup>* mice. Cre enzyme was induced by intraperitoneal injections of 200  $\mu$ l  $\beta$ -naphthoflavone (10 mg ml<sup>-1</sup>; Sigma Aldrich) dissolved in corn oil for three consecutive days.

### Crypt isolation, cell dissociation and culture

Described previously<sup>2,4</sup>. For culture/sorting experiments, at least 3 independent experiments were performed. For each experiment, crypts/cells were pooled from 3 intestines. For microarray, sorted cells from 10 intestines were pooled. Crypts were directly

cultured as previously described (100 crypts/well on 24-well plate)<sup>4</sup>. For single-cell or doublet-cell culture, crypts were dissociated with TrypLE express (Invitrogen) including 2000 U/ml DNase (Sigma) for 30 min at 37 °C or 2 hr at room temperature. For reassociation assay from established crypt organoids, the samples were dissociated with TrypLE express for 15 min at 37 °C. Dissociated cells were passed through 20- $\mu$ m cell strainer (Celltrix) and washed with PBS. Cells were stained with PE- conjugated anti-CD24 antibody (eBioscience) and APC- conjugated anti-Epcam antibody (eBioscience) for 15 min at 4 °C, and analyzed by MoFlo (DakoCytomation). Viable epithelial single-cells or doublets were gated by forward scatter, side scatter and pulse-width parameter, and negative staining for propidium iodide or 7-ADD (eBioscience). Sorted cells were collected, pelleted, and embedded in Matrigel (BD bioscience), followed by seeding on 96-well plate (30-50 singlets or doublets/10  $\mu$ l Matrigel/well. Culture medium (Advanced DMEM/F12 supplemented with Penicillin/Streptomycin, 10 mM HEPES, Glutamax, 1 $\times$  N2, 1 $\times$  B27 (all from Invitrogen), and 1  $\mu$ M N-acetylcysteine (Sigma) containing growth factors: 50 ng/ml EGF, 100 ng/ml noggin, 1  $\mu$ g/ml R-spondin) were overlaid. Y-27632 (10  $\mu$ M) was included for the first 2 days to avoid anoikis. Growth factors were added every other day and the entire medium was changed every 4 days. In some experiments, 100 ng/ml Wnt-3a (Millipore) was added in the culture medium. Sorted cells were manually inspected by inverted microscopy, and the numbers of viable organoids in triplicate were calculated.

### Reassociation assay

500 Sorted Lgr5-GFP<sup>hi</sup> stem cells (purity >99%) were cocultured with 500 genetically unmarked CD24<sup>+</sup> Paneth cells (purity >95%). Cells were resuspended in 100  $\mu$ l of culture medium in Ultra-low attachment 96 well round-bottom plates (Corning) and the plate was left on ice for 15 min. The plate was then centrifuged (300g) for 5 min and 10  $\mu$ l of Matrigel was added in each well. For Suppl Movie 2, Lgr5-GFP<sup>hi</sup>/Confetti-RFP<sup>+</sup> and Lgr5-GFP<sup>hi</sup>/Confetti-YFP<sup>+</sup> stem cells were sorted separately from *Lgr5-EGFP-Ires-CreERT2*  $\times$  *R26R-confetti* mice<sup>2</sup>, tamoxifen-induced three days prior to sacrifice of the mice. After ten days of culture, 1500 Lgr5-GFP<sup>hi</sup>/CD24<sup>dim</sup>/Confetti-RFP<sup>+</sup> stem cells and 1500 CD24<sup>hi</sup>/Confetti-YFP<sup>+</sup> Paneth cells were sorted from these two respective organoid cultures, and filmed for ten consecutive days, interrupted twice for exchange of medium. The fluorescent and phase contrast images were acquired every 20 min by inverted microscopy (AF7000, Leica) equipped with live imaging chamber (humidified with sterile water and maintained at 37 °C, 7.5% CO<sub>2</sub>).

### Microarray analysis

Single Lgr5-GFP<sup>hi</sup> cells or Paneth cells were sorted into Buffer RLT in RNeasy Micro Kit (Qiagen). Microarray analysis (Agilent) was performed as previously described<sup>4</sup>. The data will be deposited to the GEO database. Heatmaps were created using Treeview software.

### Histology, immunohistochemistry and in situ hybridization

Samples taken from the middle of the small intestine were fixed in 4% paraformaldehyde (PFA), embedded in paraffin, and processed as previously described<sup>1</sup>. The primary antibodies were; mouse anti-E-cadherin (1:100, BD transduction), mouse anti-Ki67 (1:250, Monosan), mouse anti-phospho Histone H3 (1:1000, Millipore), rabbit anti-Sox9 (1:600, Millipore), rabbit anti-Lysozyme (1:1000, Dako) and anti-Chromogranin A (1:100, Santa Cruz). The secondary antibodies were peroxidase-conjugated antibodies or Alexa 568-conjugated antibodies. For whole-mount immunostaining, freshly isolated crypts were fixed with 4% PFA, and stained with anti-CD24 antibody (eBioscience) over night at 4 °C. After washing, the samples were incubated with Alexa 568-conjugated anti-Rat antibody over night at 4 °C. DNA was stained by DAPI (Molecular Probe). For counting the number of Lgr5 stem cells (GFP) and Paneth cells (lysozyme), 1 cm<sup>2</sup> of PFA fixed intestinal wall was

put in a mold. Four percent low melting point agarose (40°C) was added and allowed to cool on ice. Once solid, a vibrating microtome (HM650, Microm) was used to make semi-thick sections (150 µm) (velocity: 1 mm/s, frequency: 65 Hz, amplitude: 0.9 mm)<sup>2</sup>. Sections were permeabilized and stained as previously described<sup>4</sup>. Images were acquired with confocal microscopy (Leica, SP5). For in situ hybridization, cRNA probes were generated from full-length cDNA expression vectors (IMAGE consortium or RPZD) with in vitro transcription. The protocol was described elsewhere<sup>12</sup>. X-gal staining was performed as previously described<sup>4</sup>.

## Supplementary Material

Refer to Web version on PubMed Central for supplementary material.

## Acknowledgments

We thank H. Begthel, J. Korving and S. van den Brink for technical assistance, and J. Gordon for providing small intestinal sections from Cr2-tox177 mice, Lawrence Lum for providing IWP1 and Arie Abo for R-spondin1.

## References

1. Barker N, et al. Identification of stem cells in small intestine and colon by marker gene Lgr5. *Nature*. 2007; 449:1003–7. [PubMed: 17934449]
2. Snippert HJ, et al. Intestinal Crypt Homeostasis Results from Neutral Competition between Symmetrically Dividing Lgr5 Stem Cells. *Cell*. 2010; 143:134–144. [PubMed: 20887898]
3. Porter EM, Bevins CL, Ghosh D, Ganz T. The multifaceted Paneth cell. *Cell Mol Life Sci*. 2002; 59:156–70. [PubMed: 11846026]
4. Sato T, et al. Single Lgr5 stem cells build crypt-villus structures in vitro without a mesenchymal niche. *Nature*. 2009; 459:262–5. [PubMed: 19329995]
5. Garabedian EM, Roberts LJ, McNevin MS, Gordon JI. Examining the role of Paneth cells in the small intestine by lineage ablation in transgenic mice. *J Biol Chem*. 1997; 272:23729–40. [PubMed: 9295317]
6. Van der Flier LG, et al. The Intestinal Wnt/TCF Signature. *Gastroenterology*. 2007; 132:628–32. [PubMed: 17320548]
7. Altmann GG. Morphological observations on mucus-secreting nongoblet cells in the deep crypts of the rat ascending colon. *Am J Anat*. 1983; 167:95–117. [PubMed: 6869312]
8. van Es JH, et al. Notch/gamma-secretase inhibition turns proliferative cells in intestinal crypts and adenomas into goblet cells. *Nature*. 2005; 435:959–63. [PubMed: 15959515]
9. Fre S, et al. Notch signals control the fate of immature progenitor cells in the intestine. *Nature*. 2005; 435:964–8. [PubMed: 15959516]
10. van Es JH, de Geest N, van de Born M, Clevers H, Hassan BA. Intestinal stem cells lacking the Math1 tumour suppressor are refractory to Notch inhibitors. *Nature Communication*. 2010; 1:1–5.
11. van der Flier LG, et al. Transcription factor achaete scute-like 2 controls intestinal stem cell fate. *Cell*. 2009; 136:903–12. [PubMed: 19269367]
12. Gregorieff A, et al. Expression pattern of Wnt signaling components in the adult intestine. *Gastroenterology*. 2005; 129:626–38. [PubMed: 16083717]
13. Poulsen SS, Nexø E, Olsen PS, Hess J, Kirkegaard P. Immunohistochemical localization of epidermal growth factor in rat and man. *Histochemistry*. 1986; 85:389–94. [PubMed: 3536807]
14. Binnerts ME, et al. R-Spondin1 regulates Wnt signaling by inhibiting internalization of LRP6. *Proc Natl Acad Sci U S A*. 2007; 104:14700–5. [PubMed: 17804805]
15. Lustig B, et al. Negative feedback loop of Wnt signaling through upregulation of conductin/axin2 in colorectal and liver tumors. *Mol Cell Biol*. 2002; 22:1184–93. [PubMed: 11809809]
16. van de Wetering M, et al. The beta-catenin/TCF-4 complex imposes a crypt progenitor phenotype on colorectal cancer cells. *Cell*. 2002; 111:241–50. [PubMed: 12408868]

17. Moser AR, Pitot HC, Dove WF. A dominant mutation that predisposes to multiple intestinal neoplasia in the mouse. *Science*. 1990; 247:322–4. [PubMed: 2296722]
18. Chen B, et al. Small molecule-mediated disruption of Wnt-dependent signaling in tissue regeneration and cancer. *Nat Chem Biol*. 2009; 5:100–7. [PubMed: 19125156]
19. Shroyer NF, Wallis D, Venken KJ, Bellen HJ, Zoghbi HY. Gfi1 functions downstream of Math1 to control intestinal secretory cell subtype allocation and differentiation. *Genes Dev*. 2005; 19:2412–7. [PubMed: 16230531]
20. Mori-Akiyama Y, et al. SOX9 is required for the differentiation of paneth cells in the intestinal epithelium. *Gastroenterology*. 2007; 133:539–46. [PubMed: 17681175]
21. Bastide P, et al. Sox9 regulates cell proliferation and is required for Paneth cell differentiation in the intestinal epithelium. *J Cell Biol*. 2007; 178:635–48. [PubMed: 17698607]
22. Bjerknes M, Cheng H. Cell Lineage metastability in Gfi1-deficient mouse intestinal epithelium. *Dev Biol*.
23. Ireland H, et al. Inducible Cre-mediated control of gene expression in the murine gastrointestinal tract: effect of loss of beta-catenin. *Gastroenterology*. 2004; 126:1236–46. [PubMed: 15131783]
24. Ireland H, Houghton C, Howard L, Winton DJ. Cellular inheritance of a Cre-activated reporter gene to determine Paneth cell longevity in the murine small intestine. *Dev Dyn*. 2005; 233:1332–6. [PubMed: 15937933]
25. Morrison SJ, Spradling AC. Stem cells and niches: mechanisms that promote stem cell maintenance throughout life. *Cell*. 2008; 132:598–611. [PubMed: 18295578]
26. Voog J, D'Alterio C, Jones DL. Multipotent somatic stem cells contribute to the stem cell niche in the *Drosophila* testis. *Nature*. 2008; 454:1132–6. [PubMed: 18641633]
27. Bjerknes M, Cheng H. The stem-cell zone of the small intestinal epithelium. I. Evidence from Paneth cells in the adult mouse. *Am J Anat*. 1981; 160:51–63. [PubMed: 7211716]
28. Bjerknes M, Cheng H. The stem-cell zone of the small intestinal epithelium. III. Evidence from columnar, enteroendocrine, and mucous cells in the adult mouse. *Am J Anat*. 1981; 160:77–91. [PubMed: 7211718]
29. Kim KA, et al. R-Spondin proteins: a novel link to beta-catenin activation. *Cell Cycle*. 2006; 5:23–6. [PubMed: 16357527]

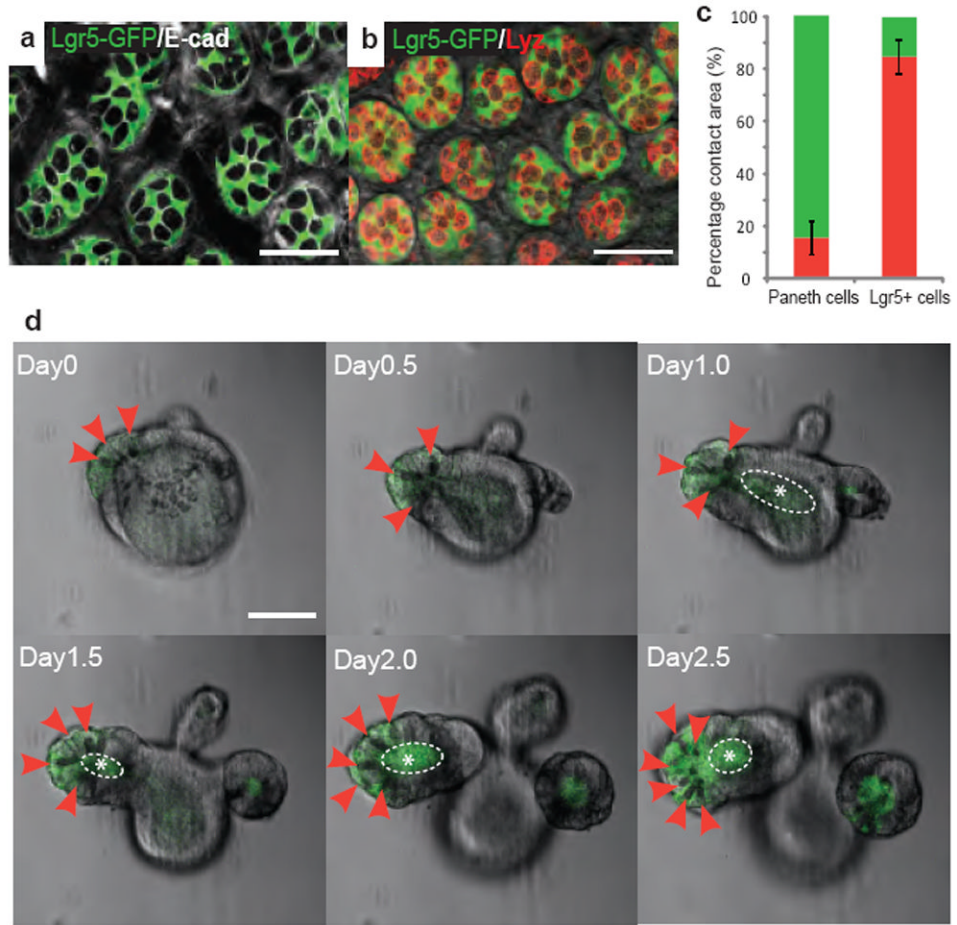


**Figure 1. Geometric distribution pattern of Paneth cells and Lgr5 stem cells**

**a,b:** Confocal cross section of *Lgr5-EGFP-ires-CreERT2* intestine. E-cadherin (a: white) demarcates cell borders. Lgr5 stem cells (green) and Paneth cells (a, black; b, lysozyme: red). **c:** Contact area of either Paneth cells or Lgr5 cells was quantified with Image J. The values are depicted as mean  $\pm$  standard deviation from three independent mice. Red columns and green columns indicate contact area with Paneth cells and Lgr5 stem cells, respectively. **d:** Stills from Suppl Movie 1. Time course of crypt organoid growth. Differential interference contrast image reveals granule-containing Paneth cells (red arrowheads) at the site of budding where a new crypt forms. Lgr5-GFP (green) stem cells expand at crypt base in close proximity to Paneth cells. \*: autofluorescence. Scale bar: 50  $\mu$ m

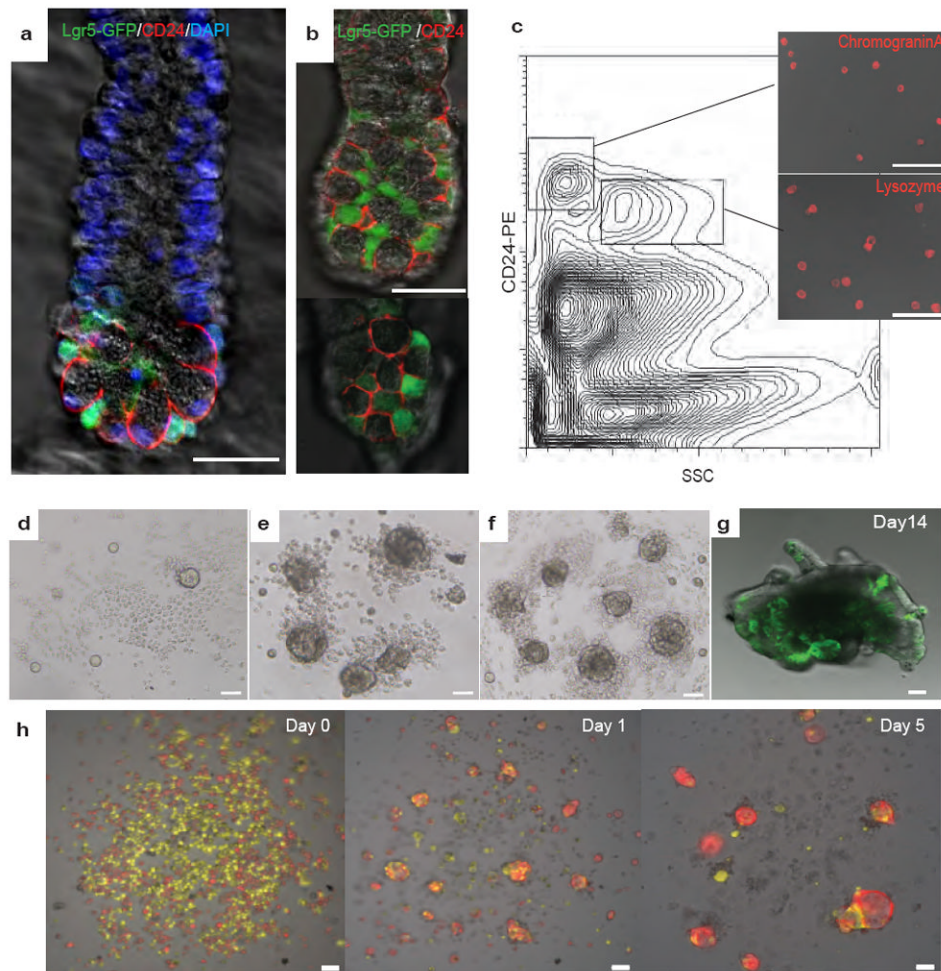


**Figure 2. Paneth cells express CD24 and support growth of Lgr5 stem cells**

**a:** Isolated small intestinal crypt. CD24 (red) is expressed by Paneth cells in which granules are visualized by differential interference contrast. Lgr5-GFP<sup>+</sup> stem cells (green). Counterstain: DAPI (blue). **b:** Isolated colonic crypt. CD24<sup>+</sup> cells (red) are in intimate contact with Lgr5 stem cells (green). Top: longitudinal crypt section; bottom: section through crypt bottom **c:** FACS plot of dissociated single cells from small intestinal crypts. Two CD24 bright populations differ by side-scatter (SSC) pattern. Sorted CD24<sup>hi</sup>/SSC<sup>low</sup> and CD24<sup>hi</sup>/SSC<sup>hi</sup> cells are subsequently stained. CD24<sup>hi</sup>/SSC<sup>low</sup> cells are positive for the enteroendocrine marker Chromogranin A (top right), while CD24<sup>hi</sup>/SSC<sup>hi</sup> cells are positive for the Paneth marker Lysozyme (bottom right). **d-g:** Single sorted Lgr5 stem cells from *Lgr5-EGFP-ires-CreERT2* small intestine (**d**), Sorted single Paneth cells (**e**) from wild type small intestine and a combination of the two cell types (**f**) were seeded in round-bottom wells and cultured for 2 days. **g:** Lgr5 stem cells form expanding Lgr5-GFP<sup>+</sup> (green) organoids only when reassociated with Paneth cells. **h:** Stills from Suppl Movie 2. Time course of the reassociation culture with RFP<sup>+</sup> Lgr5-GFP stem cells (red) and YFP<sup>+</sup> Paneth cells (yellow). Scale bar: 50  $\mu$ m.

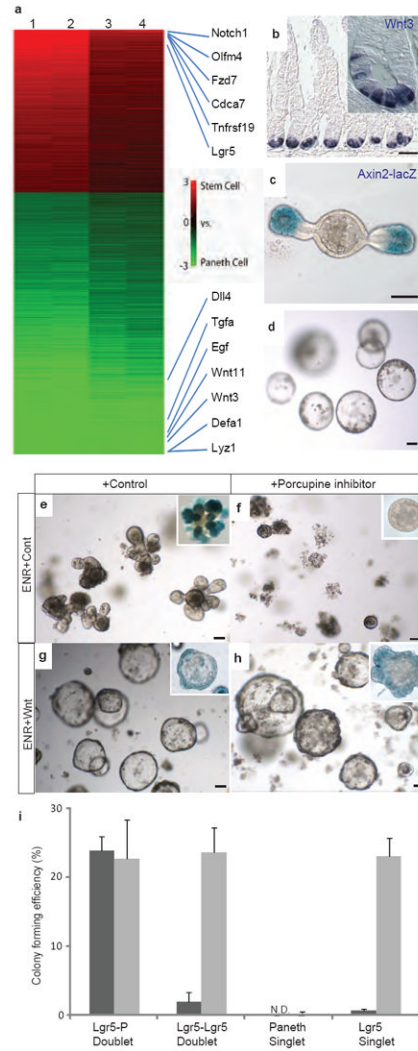


**Figure 3. Paneth cells produce Wnt3 and other essential niche signals for Lgr5 stem cells**  
**a:** Heatmap of two independent microarray expression experiments (1/2 and 3/4) performed with dye-swap (1 vs 2 and 3 vs 4) from sorted Paneth cells vs Lgr5 stem cells. **b:** *Wnt3* is expressed by Paneth cells at crypt bottoms as analyzed by in situ hybridization, **c-h:** Localized Wnt production regulates crypt-villus morphogenesis in culture. **c:** Freshly isolated crypts from *Axin2-lacZ* mouse were cultured in standard EGF/Noggin/Rspondin1 medium (ENR) medium for 4 days. LacZ response is only seen near the bottoms of the two crypts. **d:** Intestinal adenoma samples from *Apc<sup>min</sup>* mice were cultured in ENR medium in the absence of R-spondin for 7 days. **e:** Axin2-LacZ crypts grown in ENR medium. **f:** As in **e**) with the addition of porcupine inhibitor IWP1 at 1  $\mu$ M. **g:** Crypts from *Axin2-LacZ* mouse cultured in ENR medium plus Wnt3a **h:** same as **g**) with the addition of IWP1. Insets in **e-h** depict Axin2-LacZ expression (blue). **e, g, h:** 6 days culture. **f:** 3 days culture after which the organoids disintegrate. See also Suppl Fig 2. **i:** Plating efficiency of Lgr5 stem cell-Paneth doublets, Lgr5 stem cell doublets, single Paneth cells and single Lgr5 stem cells with (grey) or without (black) Wnt-3A at 100 ng ml<sup>-1</sup>. Assays were read out as budding organoids at 14 days after sorting. The values are depicted as mean $\pm$ standard error of the mean (SEM) from three independent experiments. N.D.; not detected. See also Suppl Fig 3 and online methods for detail of doublet isolation and culture.

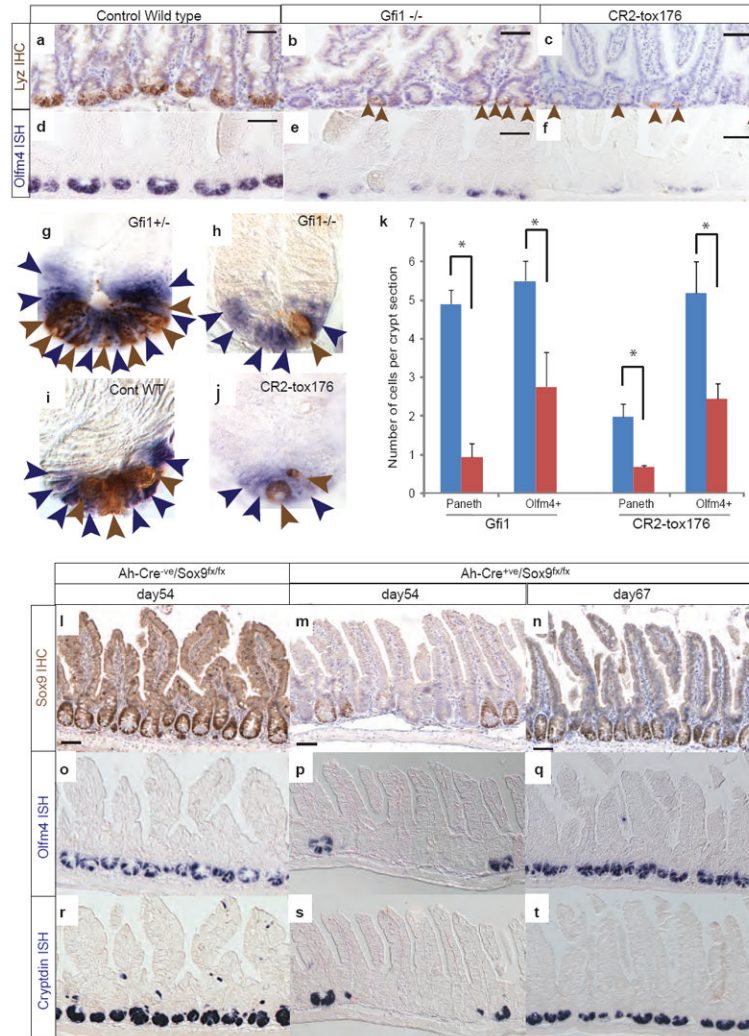


**Figure 4. Paneth cells regulate numbers of intestinal stem cells *in vivo***  
**a-k:** Paneth cells and stem cells in constitutive models of Paneth cell decrease. **a-c:** lysozyme stain (brown arrowheads indicate positive cells) and **d-f:** *Olfm4* staining of crypts of adult (6-7 week-old) mice of the indicated genotypes. **g-j:** double stain, lysozyme (brown), *Olfm4* (blue) of a representative crypt of the indicated genotype. Brown and blue arrowheads indicate Paneth cells and stem cells, respectively. **k:** Quantification of stem and Paneth cell numbers in both models. For each bar, 100 crypts were scored for each of three mice. Mutant mice (red) and their control mice (blue). \*:  $p < 0.01$ . **l-t:** Paneth cells and stem cells in inducible Paneth cells depletion model. Mice indicated genotypes were injected with  $\beta$ -naphthoflavone to induce Cre and were analyzed 54 or 67 days after Cre induction by staining for Sox9 protein (brown), *Olfm4* or *Cryptdin* mRNA (blue). Serial sections: **i,o,r;** **m,p,s;** and **n,q,t**. See text for experimental detail. Note the absence of Paneth cells (**s**) and stem cells (**p**) in Sox9<sup>-/-</sup> crypts (**m**). Scale bar: 50  $\mu$ m